The American Journal of Pathology, Vol. 187, No. 4, April 2017

The American Journal of
PATHOLOGY
ajp.amjpathol.org

GASTROINTESTINAL, HEPATOBILIARY, AND PANCREATIC PATHOLOGY

TNFΔARE Mice Display Abnormal Lymphatics and Develop Tertiary Lymphoid Organs in the Mesentery

Sonia Rehal and Pierre-Yves von der Weid

From the Inflammation Research Network and Smooth Muscle Research Group, Department of Physiology & Pharmacology, Snyder Institute for Chronic Diseases, Cumming School of Medicine, University of Calgary, Calgary, Alberta, Canada

Accepted for publication December 1, 2016.

Address correspondence to Pierre-Yves von der Weid, Ph.D., Department of Physiology & Pharmacology, Cumming School of Medicine, University of Calgary, 3330 Hospital Dr. N.W., Calgary, Alberta, Canada T2N 4N1. E-mail: vonderwe@ucalgary.ca.

Chronic inflammatory diseases are associated with a persistent and enhanced response to environmental antigens. As an adaptive response to this exaggerated immune state, affected tissue typically develops tertiary lymphoid organs. Studies of Crohn disease (CD), a chronic inflammatory disease of the intestinal tract, report tertiary lymphoid organs present within the mucosal wall, along with other lymphatic diseases, such as lymphangiogenesis and obstructed lymphatic vessels. These observations suggest that downstream mesenteric lymphatic vessels and lymph drainage into mesenteric lymph nodes may be compromised. However, information is lacking on the morphologic features and functional status of mesenteric lymphatics in CD. Using confocal imaging, PCR, flow cytometry, and functional strategies, we addressed these questions in the established *TNFΔARE* mouse model of CD and found that this mouse model had many lymphatic abnormalities reminiscent of human CD. These abnormalities include intestinal lymphangiectasia, mesenteric lymph node lymphadenopathy, and lymphangiogenesis in both the mesentery and mucosa. Critically, *TNFΔARE* mice also present mesenteric tertiary lymphoid organs and have altered lymphatic transport of dendritic cells to mesenteric lymph nodes, two features likely to actively modulate immunity. Our findings provide key insights into lymphatic remodeling in the *TNFΔARE* mouse model. They shed light on the involvement of these lymphatic changes in immune dysfunctions observed in CD and suggest the lymphatic system as new target for therapeutic options. *(Am J Pathol 2017, 187: 798–807; http://dx.doi.org/10.1016/j.ajpath.2016.12.007)*

Crohn disease (CD) is an inflammatory bowel disease that results in chronic inflammation of the intestine. CD epidemiology suggests a multifactorial pathogenesis, which unfortunately limits successful therapeutic options. Chronic inflammation, prominent in the disease process, points to an abnormal clearing of immune cells via the mesenteric lymphatic system. In fact, defects in lymphatic morphologic features in the small intestine have been reported in patients with CD[1–7] and in recapitulating mouse models.[8,9] Specifically, lymphangiogenesis, obstructed lymphatic vessels, extensive dilation of lacteals and submucosal lymphatics and/or their occlusion by lymphocytic thrombi, and granulomas have been reported.[1–7] Similar to other chronic inflammatory diseases, tertiary lymphoid organs (TLOs) develop in the intestinal mucosa of patients with CD.[10–13] Although incompletely characterized in these studies, these TLOs appear to have useful diagnostic value.[10–13] TLOs are thought to appear in diseases with sustained immune activation, such as during chronic inflammation, and form as a result of distinct signaling pathways.[14] Their development involves the interplay between immune and stromal cells. Most importantly, lymphotoxin β-receptor

Supported by NIH grant HL096552, Canadian Institutes of Health Research grant MOP89975, and the Lymphedema Research and Education Program, Snyder Institute for Chronic Diseases, Cumming School of Medicine, University of Calgary (P.-Y.v.d.W.).

Disclosures: None declared.

http://dx.doi.org/10.1016/j.ajpath.2016.12.007

(LTβR) expressed on stromal cells and its interaction with $LT\alpha_2\beta_2$ released by hematopoietic cells drives the formation of new lymphoid organs.[14] Other players in TLO development include intercellular, vascular, and addressin cell adhesion molecules (intercellular adhesion molecule 1, vascular cell adhesion molecule 1, and mucosal vascular addressin cell adhesion molecule 1, respectively) and chemokines, such as chemokine (C-C motif) ligand (CCL)-19 and CCL21.

The aforementioned intestinal lymphatic abnormalities found during CD are likely to extend to the mesenteric lymphatic vessels and draining mesenteric lymph nodes (MLNs). Surprisingly, although a few studies have found the consequent effect of chronic intestinal inflammation on normal MLN physiologic features,[15–17] there are no reports of lymphatic abnormalities observed within the mesentery during chronic inflammation. Human mesenteric tissue is rarely examined during surgical resections, and scarce information is available about mesenteric lymphatic vascular changes occurring during inflammation.

Using the *TNFΔARE* mouse, a transgenic murine model of spontaneous CD-like ileitis, we investigated the physiology, morphology, and patency of the ileal and mesenteric lymphatic system. We report that chronic ileitis in *TNFΔARE* mice is accompanied by intestinal and mesenteric lymphatic anomalies, such as lymphadenopathy, lymphangiectasia, lymphangiogenesis, and compromised lymphatic transport function and permeability. Importantly, we observed that TLOs develop in the mesentery of *TNFΔARE* mice, which appear to be functional components of the immune response. These findings further validate the *TNFΔARE* mouse model as a useful model to study CD-ileitis pathogenesis because it replicates lymphatic abnormalities seen in the human disease. This study offers further insight into the lymphatic drainage and immune cell trafficking abnormalities in CD.

Materials and Methods

Animals

TNFΔARE mice were originally developed and characterized by Kontoyiannis et al.[18] All experiments were performed on 24- to 28-week-old mice and in accordance with the Canadian Council on Animal Care guidelines on the use of animals in research, with ethical approval and oversight by the University of Calgary Health Science Animal Care Committee.

Characterization of Ileitis

Macroscopic Damage

Severity of ileum inflammation was assessed according to scoring criteria adapted from Elsheikh et al,[19] where ulceration, adhesions, hyperemia, and bleeding were scored with values from 0 to 2, up to a maximum total score of 8.

Weight Loss

Differences in weight were measured as absolute body weight.

Myeloperoxidase Activity

Terminal ileum tissue was assessed for myeloperoxidase activity as previously published.[20]

Histologic Analysis

Tissue samples were fixed in neutral-buffered formalin, embedded in paraffin, sectioned and stained with hematoxylin and eosin, and then examined by light microscopy (Dmi1 Stereomicroscope, Leica, Ontario, Canada).

Assessment of Lipid Transport and Integrity Functions

Bodipy (Thermo Fisher Scientific, Waltham, MA) mixed with olive oil (20 μL/200 μL) was administered by oral gavage. Animals were sacrificed 1 hour later and tissues homogenized in 1 mL of Dulbecco's phosphate-buffered saline (DPBS) (Sigma-Aldrich, St. Louis, MO). Fluorescence was measured in tissue lysates and blood with a spectrophotometer (PerkinElmer, Waltham, MA) and normalized to protein content (Precision Red Advanced Protein Reagent, Cytoskeleton Inc., Denver, CO). Bodipy leakage (lymphatic vessel integrity) was assessed in *ex vivo* preparations of bodipy gavaged mice. A mid-abdominal incision was made, and the terminal small intestinal loop was exposed onto gauze that was kept wet with phosphate-buffered saline (PBS) (Sigma-Aldrich). A viewing window of the mesenteric arcade was made and visualized for fluorescence. Bodipy-filled mesenteric lymphatic vessels were identified and imaged with a fluorescent stereomicroscope (EL6000; Leica, Wetzlar, Germany).

Quantitative Real-Time PCR

Primers for target cDNA are listed in Table 1. Real-time amplification of target transcripts was performed using EvaGreen qPCR Mastermix (Diamed, Mississauga, ON, Canada) in an ABI StepOne Plus PCR System (Thermo Fisher Scientific). Annealing temperature used was 55°C, and 40 cycles were used to amplify sufficient amplicon product.

Immunofluorescence

Whole Mount Immunofluorescence

Mesenteries pinned on sylgard (Dow Corning, Midland, MI) were fixed in 10% formalin for 2 hours, washed with DPBS, permeabilized for 2 hours with 0.3% Triton X-100/PBS, and subsequently blocked with 5% normal

Table 1 Primer Sequences

Transcript	Forward	Reverse	Product size, bp
LTβR	5′-TGGTGCTCATCCCTACCTTC-3′	5′-CACACCTCCTCTCAAACCCT-3′	127
VEGFR-3	5′-CTGGCAAATGGTTACTCCATGA-3′	5′-ACAACCCGTGTGTCTTCACTG-3′	103
PROX-1	5′-TACCAGGTCTACGACAGCACCG-3′	5′-GTCTTCAGACAGGTCGCCATC-3′	108
LYVE-1	5′-CAGCACACTAGCCTGGTGTTA-3′	5′-CGCCCATGATTCTGCATGTAGA-3′	111
CCL19	5′-GATCGCATCATCCGAAGACT-3′	5′-TTCTGGTCCTTGGTTTCCTG-3′	123
CCL21	5′-ATGTGCAAACCCTGAGGAAG-3′	5′-TTAGAGGTTCCCCGGTTCTT-3′	113

CCL19, chemokine (C-C motif) ligand 19; CCL21, chemokine (C-C motif) ligand 21; LTβR, lymphotoxin β-receptor; LYVE-1, lymphatic vessel endothelial hyaluronan receptor 1; PROX-1, prospero homeobox protein 1; VEGFR-3, vascular endothelial growth factor 3.

serum and 1% bovine serum albumin (BSA) for 2 hours. Primary antibody incubation took place overnight at 4°C in 0.3% Triton X-100/PBS. Tissues were incubated for 2 hours with secondary antibody incubation followed by thorough washes with 0.3% Triton X-100/PBS. Mesenteries were spread on to coverslides and coverslip with mounting media (Fluorsave; VWR International, Radnor, PA) and imaged within 24 hours (TCS SP8 Confocal Microscope; Leica Microsystems, Richmond Hill, ON, Canada).

Paraffin-Embedded Immunofluorescence

Briefly, sections were deparaffinized and a sodium citrate buffer/steamer technique was used for antigen retrieval. Sample slides were washed with 0.025% Triton X-100/PBS and blocked in 10% normal serum with 1% BSA in PBS for 2 hours. Primary antibody incubation took place overnight at 4°C in 1% BSA/PBS at 1/100. Secondary antibody incubation was performed in 1% BSA/0.025% Triton X-100/PBS at a 1/250 concentration. Slides were washed and mounting media (Fluorsave) was used under the coverslip. Samples were imaged within 24 hours.

Flow Cytometry

Single-cell suspensions from MLNs and mesenteric TLOs were harvested from both WT and *TNFΔARE* mice and collected in cold suspension buffer (RPMI 1640 medium, 5% forward scatter, 2 mmol/L EDTA, penicillin streptomycin). Tissues were disrupted using the gentleMACS Dissociator (Miltenyi Biotec, Auburn, CA) and filtered and washed through a 40-μm nylon filter (BD Biosciences, Mississauga, ON, Canada). All flow cytometry staining was incubated with conjugated antibodies for 1 hour at 4°C and subsequently washed and prepared in cold FACS buffer (PBS, 1% BSA, 0.1% sodium azide). The cells were analyzed using Attune Acoustic Focusing Cytometer (Life Technologies, Carlsbad, CA) and data generated using FlowJo (Tree Star, Ashland, OR).

Cell Labeling Experiments

Bone marrow–derived dendritic cells (DCs) from wild-type (WT) and CCR7 knockout (KO) mice (kindly gifted by Dr. Paul Kubes, University of Calgary, Calgary, Alberta, Canada) were harvested and seeded at 5×10^6/10 mL in RPMI 1640 medium (Sigma-Aldrich) supplemented with 10% FBS, 20 mmol/L HEPES, 2% penicillin streptomycin, 1% GlutaMAX, 51% sodium pyruvate (all Gibco, Grand Island, NY), and recombinant murine granulocyte-macrophage colony-stimulating factor (20 ng/mL; Peprotech, Rocky Hill, NJ). Cells were refed with 20 ng/mL of granulocyte-macrophage colony-stimulating factor and 10 mL of medium on day 3 and day 6. Cells were harvested on day 8 and resuspended in 90% fetal bovine serum and 10% dimethyl sulfoxide and stored in liquid nitrogen. Cells were subsequently thawed, washed, resuspended, and labeled with either carboxyfluorescein succinimidyl ester for WT DCs or Deep Red (Thermo Fisher Scientific) for CCR7 KO DCs. For cell transfer, 1×10^6 cells of each WT and CCR7 KO DCs were washed three times in sterile DPBS, resuspended in 500 μL of DPBS, and administered i.p. For intestinal DC trafficking, mice were orally gavaged with 100 μg of ovalbumin, conjugated to Alexa Fluor 647 (Thermo Fisher Scientific) 1 hour before analysis by flow cytometry.

Antibodies

Antibodies against podoplanin, CCL21, peripheral node addressin (PNAd)-1, major histocompatibility complex (MHC)-II, Cd11c, CD103, plasmacytoid dendritic cell antigen (pDCA)-1, and CX3C chemokine receptor 1 (CX_3CR_1) were obtained from Ebioscience (San Diego, CA), vascular endothelial growth factor receptor (VEGFR)-3 from Lifespan (Providence, RI), α-smooth muscle actin from Sigma-Aldrich, prospero homeobox protein (PROX)-1 and Ki-67 from Abcam (Toronto, ON, Canada), LTβR from Biolegend (San Diego, CA), and CD3 from BD Biosciences. Isotype control antibodies were purchased as recommended by the respective antibody provider.

Statistical Analysis

Data are expressed as means ± 1 SEM. Sample size varied from 4 to 12. Statistical significance was assessed using a two-tailed unpaired *t*-test for parametric data, whereas the

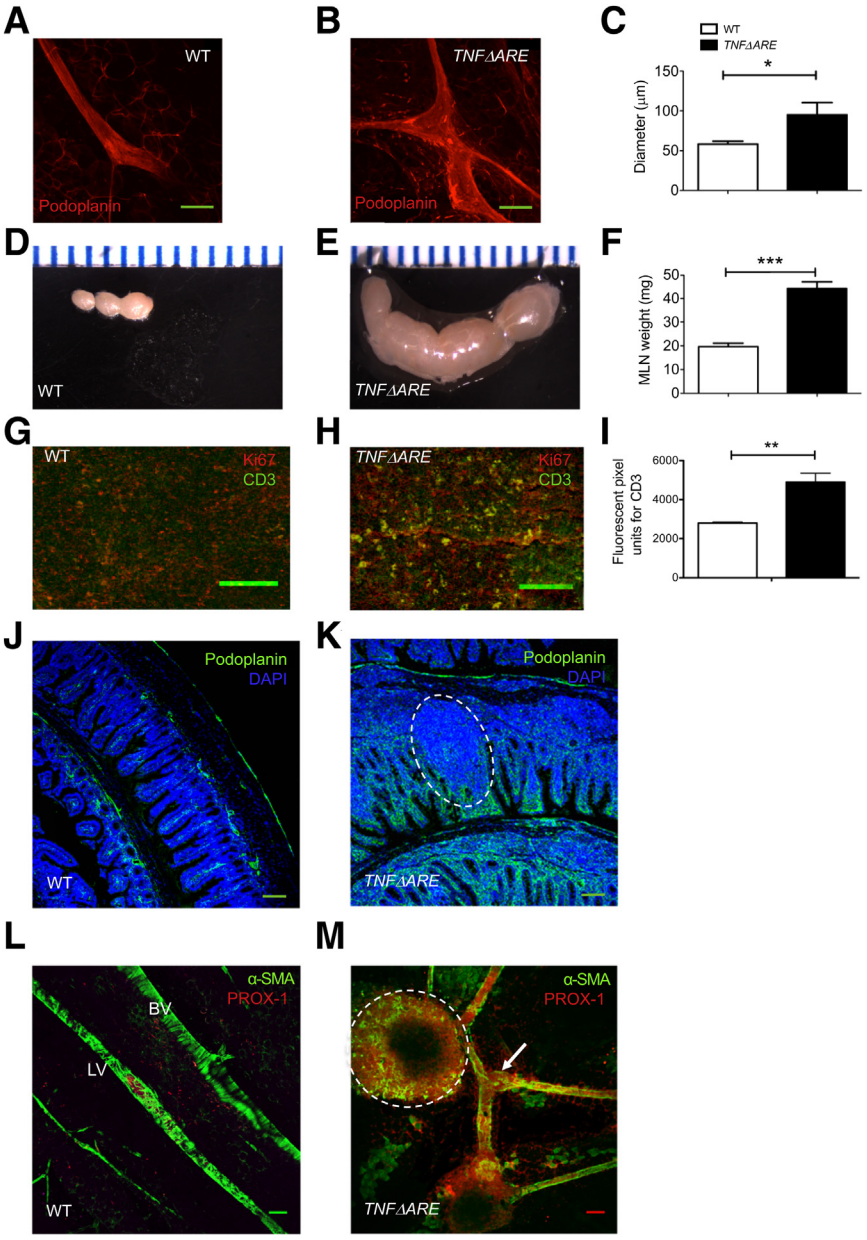

Figure 1 Chronic ileitis in *TNFΔARE* mice is associated with lymphangiectasia, lymphadenopathy, and lymphangiogenesis. **A** and **B:** Representative confocal immunofluorescence images of collecting lymphatic vessels stained with podoplanin antibody in wild-type (WT) (**A**) and *TNFΔARE* (**B**) mouse mesentery, where enlarged lymphatic vessels representing lymphangiectasia can be seen. **C:** Quantification of lymphatic vessel diameters in WT and *TNFΔARE* mouse mesentery obtained from whole mount immunostaining of mesenteric lymphatic vessels stained for podoplanin. **D**—**F:** WT mesenteric lymph nodes (MLNs) and observed lymphadenopathy in *TNFΔARE* MLNs (**E**) scaled alongside a ruler and quantified by dry weight (**F**). **G**—**I:** Increased cellularity and lymphocyte proliferation in *TNFΔARE* MLNs as assessed by the expression of Ki-67, a proliferation marker, and CD3, a lymphocyte marker (**G** and **H**) and quantified by measurement of CD3 fluorescence intensity (**I**). **J** and **K:** Intestinal lymphangiogenesis shown on staining of WT (**J**) and *TNFΔARE* (**K**) terminal ileum Swiss roll sections, with podoplanin and DAPI. In WT ileum, phenotypical lacteals infiltrating each intestinal villi converge into vessels within the lamina propria. In contrast, *TNFΔARE* ileum have massive expansion of podoplanin-positive tortuous and extremely unorganized vessels. Merging of vessels in the lamina propria is anarchic, possibly compromising the directionality of lymph flow. Furthermore, lymphoid aggregate (**white dashed circle**) and general destruction of villus structure in *TNFΔARE* mucosa are observed by DAPI nuclear staining (or absence thereof, respectively). Mesenteric lymphangiogenesis as observed in whole mount stained for α-smooth muscle actin (α-SMA) and prospero homeobox protein (PROX)-1. **L:** WT mesentery shows PROX-1—positive collecting lymphatic vessels (LVs) well aligned along a main mesenteric blood vessel (BV) and displaying a rather uniform coverage of lymphatic muscle cells. **M:** *TNFΔARE* mesentery exhibits lymphatic vessels, with numerous branches, less organized lymphatic muscle cells coverage, and large bulbous valves (**arrow**), suggesting engorgement with lymph. A tertiary lymphoid organ (TLO), indicated with **white dashed circle**, is seen intricately connected to the lymphatic vessels. Data are expressed as means ± SEM. $*P < 0.05$, $**P < 0.01$, $***P < 0.001$. Scale bars = 100 μm (**A**, **B**, and **G**—**M**).

Mann-Whitney test was performed for nonparametric data. $P < 0.05$ was considered significant.

Results

Association of Chronic Ileitis in *TNFΔARE* Mice with Lymphangiectasia, Lymphadenopathy, and Lymphangiogenesis

Assessment of intestinal inflammation in 24-week-old *TNFΔARE* mice revealed significant weight loss associated with histologic signs of intestinal injury and increased myeloperoxidase activity (Supplemental Figure S1), confirming previous findings.[18] Previous studies have described mesenteric lymphatic vessel dilation and contractile dysfunction to correlate well with the severity of intestinal damage.[21—24] Similarly, lymphatic vessels in *TNFΔARE* mesentery were dilated, reaching twice the size of the WT vessels (Figure 1, A—C) and averaging 90 μm, a diameter comparable to that of a mesenteric artery. Other lymphatic system abnormalities, such as mesenteric lymphadenopathy, were also consistently observed, and MLNs found in *TNFΔARE* mesentery were massively enlarged (Figure 1, D—F) with a strong increase in $CD3^+$ T lymphocyte infiltrate (Figure 1, G—I). Furthermore, as illustrated in Figure 1, J and K, a significant lymphangiogenic response was observed in the ileal mucosa of *TNFΔARE* mice. Figure 1K also displays a lymphoid aggregate, commonly observed in

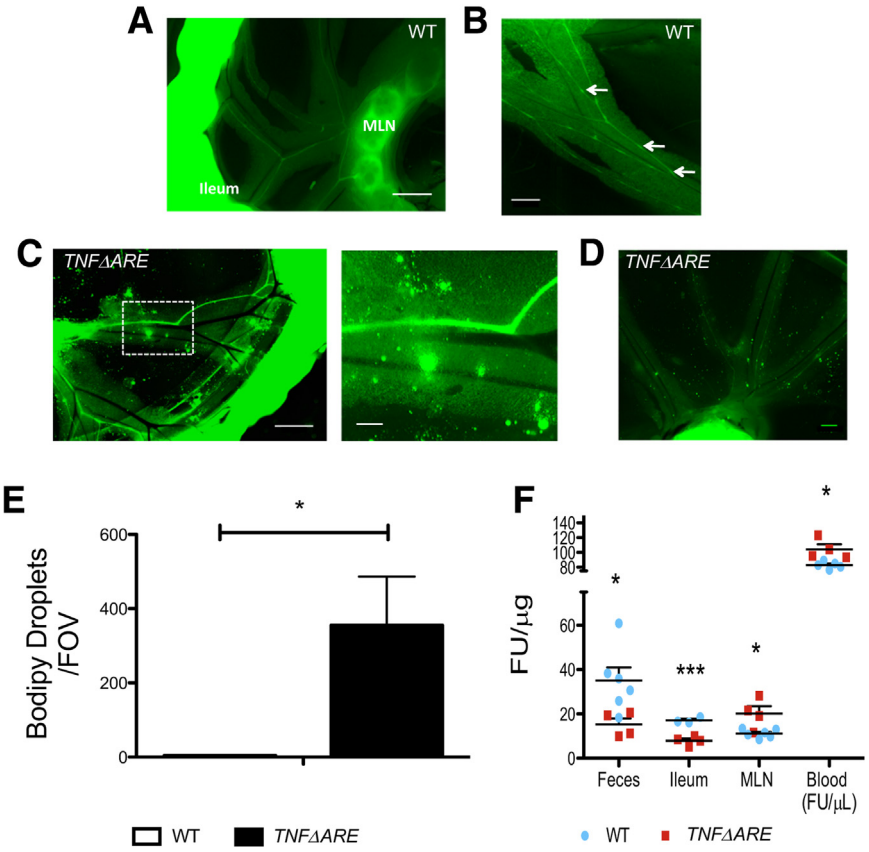

Figure 2 *TNFΔARE* mice have leaky collecting lymphatic vessels and enhanced lipid clearance. **A** and **B:** Representative image of wild-type (WT) mesentery after oral gavage with the fluorescent lipid bodipy reveals bodipy-loaded typical collecting lymphatic vessels (LVs) with phenotypical valves (**arrows**), and bodipy-loaded mesenteric lymph nodes (MLNs), suggesting efficient drainage. **C** and **D:** There are significant changes in vessel morphologic features occurring in the mesentery of *TNFΔARE* mice. Lymphatic vessels are dilated and leaky, as shown by spillage of fluorescent bodipy droplets in the nearby mesentery (magnified view of the **boxed area** is shown in the **right panel** of **C**). **E:** Quantification of the lymphatic vessel leakiness, measured by the number of bodipy droplets present in a given field of view (FOV). Images, all 7100 × 5300 μm, were assigned a threshold value for the largest and smallest droplet in the image and subsequently quantified. **F:** Overall lymphatic vessel transport function was extrapolated by measuring clearance of gavaged bodipy from feces, ileum, MLNs, and blood. Quantification depicts an overall enhanced clearance (reduced fluorescent signal) from the ileum toward the MLN and blood in *TNFΔARE*. Data are expressed as means ± SEM. $*P < 0.05$, $***P < 0.001$. Scale bars: 1 mm (**A** and **C**, **left panel**); 500 μm (**B** and **D**); 250 μm (**C**, **right panel**).

TNFΔARE ileum. Lymphangiogenesis was also preeminent in the mesentery of *TNFΔARE* mice, where new, albeit tortuous, vessels positive for α-smooth muscle actin and PROX-1 were observed (Figure 1, L and M).

Compromise of Lymphatic Lipid Transport and Integrity in *TNFΔARE* Ileum

We next measured the clearance of ingested fluorescent lipid bodipy into various tissues to examine whether lymphatic transport function was altered in *TNFΔARE* mice. Lipid clearance was substantially increased in *TNFΔARE* ileum and feces, and consequently fluorescence accumulation in MLN and blood increased (Figure 2F). These observations suggest an overall increased lipid and lymph transport from the gut to MLN and blood via the lymphatic vessels. Furthermore, we observed that although lymphatic vessels are thought to be impermeable to lymph, allowing its efficient drainage, the integrity of the *TNFΔARE* mesenteric collecting lymphatic vessels seemed compromised (Figure 2, C and D). Vessels in the *TNFΔARE* mesentery appeared dilated, as already reported above, but also leaky, allowing bodipy droplets to seep out of the vessels into the mesentery. This leakage, quantified in Figure 2E, was not observed in WT mesentery, where bodipy was tightly contained within the collecting lymphatic vessels (Figure 2, A and B).

Mesenteric TLOs in *TNFΔARE* Mice

A striking change observed in the *TNFΔARE* mesentery was the presence of follicular structure resembling TLOs (Figure 3B). These structures were easily spotted because the *TNFΔARE* mesentery lacked adiposity seen in WT mice (Figure 3A). However, imaging of WT tissues after fat clearing revealed no such structures (data not shown). Furthermore, TLOs were not observed in mesenteries from *TNFΔARE* mice younger than 24 weeks of age (data not shown). To confirm the identity of these structures, we assessed the expression of the main genes involved in TLO development and lymphangiogenesis, important for the development of lymphoid-associated lymphatic vessels. Figure 3C shows that mRNA expression of these genes was substantial in the *TNFΔARE* structures, in particular, LTβR and VEGFR-3, which were significantly up-regulated when compared with WT MLNs. The PCR data also reveal up-regulation of these genes in *TNFΔARE* MLNs, confirming their lymphadenopathic phenotype. We then used immunostaining to further confirm that the mesenteric follicles were TLOs. Figure 3D reveals LTβR-positive TLOs lining along (and wrapped by) CCL21-stained lymphatic

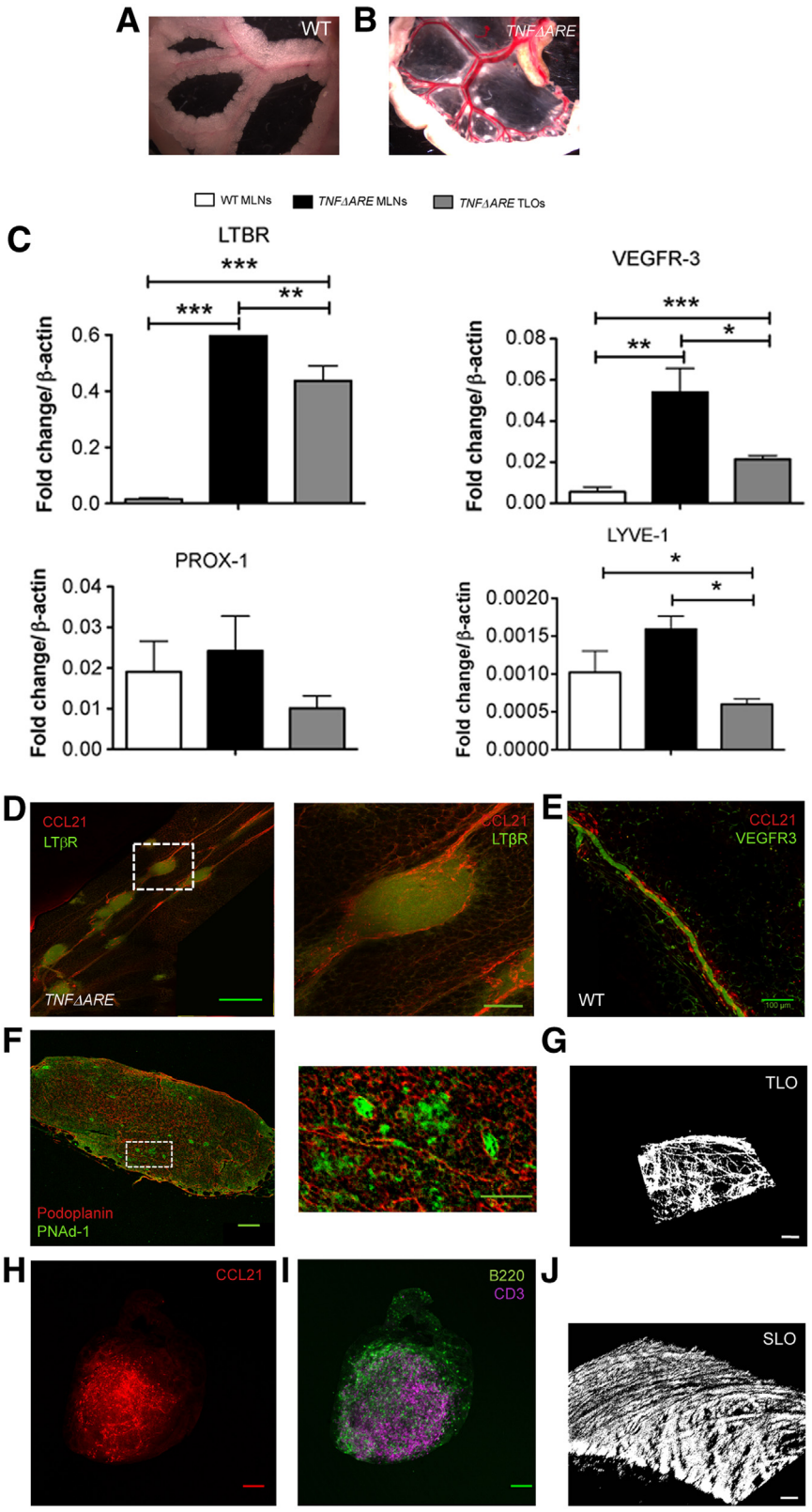

Figure 3 *TNFΔARE* mice develop mesenteric tertiary lymphoid organs (TLOs). **A** and **B:** Representative images of wild-type (WT) and *TNFΔARE* mesentery revealing small lymphoid structures along the length of a *TNFΔARE* lymphatic vessels. Notice the lack of fat investiture around the vessels and the enlarged mesenteric lymph nodes (MLNs). **C:** Differential expression of various TLO development—related genes quantified by real-time quantitative PCR. TLOs express lymphotoxin β-receptor (LTβR) and all prolymphangiogenesis genes, vascular endothelial growth factor receptor (VEGFR)-3 (*FLT4*), prospero homeobox protein (PROX)-11, and lymphatic vessel endothelial hyaluronan receptor (LYVE)-1 at levels comparable to *TNFΔARE* MLNs. Notice that VEGFR-3 and LTβR are both up-regulated in *TNFΔARE* MLNs. **D:** Representative image of TLOs aligned like beads on a string along a collecting lymphatic vessel in *TNFΔARE* mesentery. Magnified view of the **boxed area** seen in the **right panel** shows chemokine (C-C motif) ligand (CCL)-21—positive vessels wrapped around the TLO brightly stained for LTβR. **E:** Representative image of lymphatic vessels in a WT mesentery at the same magnification. **F:** Mesenteric TLOs harbor structures positive for podoplanin and peripheral node addressin (PNAd)-1 (high endothelial venule marker, see magnified view of the **boxed area** in the **right panel**). **G** and **H:** As well, they contain CCL21-positive vessels and CD3 T-cell staining and B220 B lymphocytes staining. **I** and **J:** Finally, TLOs are surrounded by collagen deposition similar to lymph nodes (SLO, mouse iliac lymph node used as example), as highlighted by second harmonic generation images. Data are expressed as means ± SEM. $^{*}P < 0.05$, $^{**}P < 0.01$, $^{***}P < 0.001$. Scale bars: 500 μm (**D**, **left panel**); 100 μm (**D**, **right panel**, **E**, **F**, **left panel**, **H**, and **I**); 50 μm (**F**, **right panel**, **G**, and **J**).

vessels like beads on strings in the *TNFΔARE* mouse mesentery, which were totally absent in WT mesentery (Figure 3E). Mesenteric TLOs possess a lymph node—like structure, staining positive for CCL21, CD3 (T cells), B220 (B cells) (Figure 3, G and H), and PNAd, a marker for high endothelial venules, which is critical in lymph node morphologic features and function[14] (Figure 3F). Furthermore, they developed a collagen-based capsule-like

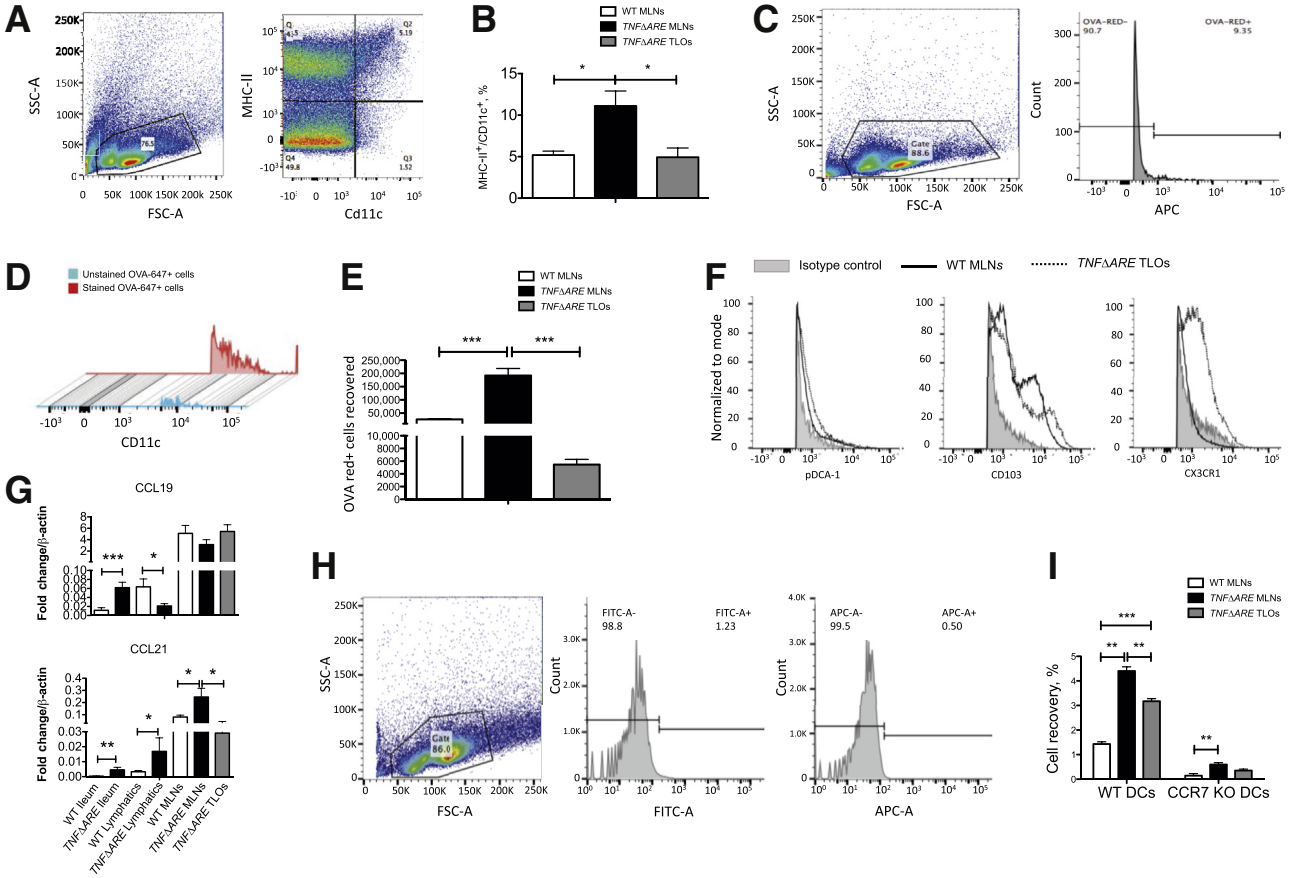

Figure 4 CX3C chemokine receptor 1 ($CX_3CR_1^+$) enriched dendritic cells (DCs) traffic to tertiary lymphoid organs (TLOs), in a CCR7-dependent manner in *TNFΔARE* mesentery. **A:** Flow cytometry gating strategy based on major histocompatibility (MHC)-II^+/$Cd11c^+$ DCs. **B:** Total DC counts quantified in wild-type (WT) mesenteric lymph nodes (MLNs), *TNFΔARE* MLNs, and *TNFΔARE* mesenteric TLOs. **C:** Gating strategy used to positively identify OVA-647^+ cells within WT MLNs, *TNFΔARE* MLNs, and *TNFΔARE* mesenteric TLOs. **D:** OVA-647^+ cells are shown to be highly positive for Cd11c (90.8% of OVA-647^+ cells, with mean fluorescence intensity three times as bright as unstained cells). **E:** Quantification of the OVA-647^+ cells sorted from WT MLNs, *TNFΔARE* MLNs, and *TNFΔARE* mesenteric TLOs. **F:** Cell surface expression of plasmacytoid dendritic cell antigen (pDCA)-1, CD103, and CX_3CR_1 in WT MLNs and *TNFΔARE* mesenteric TLOs. **G:** CCL19 and CCL21 mRNA expression in WT ileum, *TNFΔARE* ileum, WT lymphatics, *TNFΔARE* lymphatics, WT MLNs, *TNFΔARE* MLNs, and TLOs. **H:** Gating strategy used to identify positive populations of WT DCs [fluorescein isothiocyanate (FITC)] and CCR7 knockout (KO) DCs [antigen-presenting cells (APC)] in tissue. **I:** Assessment of the role of CCR7 for DC trafficking to *TNFΔARE* MLNs and *TNFΔARE* mesenteric TLOs. Bone marrow–derived DCs from WT and CCR7 KO mice were injected in 1:1 ratio i.p. 48 hours before flow analysis. Accumulation of WT and CCR7 KO DCs was quantified in WT MLNs, *TNFΔARE* MLNs, and *TNFΔARE E* mesenteric TLOs. Data are expressed as means ± SEM. $*P < 0.05$, $**P < 0.01$, $***P < 0.001$.

structure similar to lymph nodes as revealed using second harmonic generation microscopy (Figure 3, I and J).

Traffic of $C_X3CR_1^+$-Enriched DCs to *TNFΔARE* TLOs in a CCR7-Dependent Manner

To evaluate whether mesenteric TLOs were active immune structures harboring resident or migratory DCs, we performed flow cytometry experiments and revealed that a Cd11c/MHC II-positive cell population was present in mesenteric TLOs in an amount comparable to WT MLNs, whereas this population was significantly enhanced in *TNFΔARE* MLNs (Figure 4, A and B). We further investigated the trafficking of migratory DCs of intestinal origin by administering the antigen OVA-647 by oral gavage. Figure 4 C–E illustrates that *TNFΔARE* MLNs had large infiltrates of cells that were positive for OVA-647 and that a significant amount of OVA-647–carrying cells were found in mesenteric TLOs. We further examined *TNFΔARE* TLOs for cell surface expression of pDCA-1, CD103, and CX_3CR_1. We observed an enrichment of CX_3CR_1-positive DCs in *TNFΔARE* TLOs when compared with normal WT MLN DC populations (Figure 4F). We next examined their chemokine ligand expression and found that CCL19 expression was down-regulated in lymphatics and up-regulated in the ileum of *TNFΔARE* mice (Figure 4G). On the other hand, CCL21 expression was up-regulated in the ileum, lymphatics, and MLNs. CCL21 was also expressed in *TNFΔARE* TLOs at level comparable to that in WT MLNs (Figure 4G). Finally, using differentially labeled bone marrow–derived cells from WT and CCR7 KO mice, we assessed the role of

CCR7 in DC trafficking to *TNFΔARE* MLNs and mesenteric TLOs. We found that similar to trafficking to *TNFΔARE* MLNs, trafficking of DCs to TLOs was a CCR7-dependent process (Figure 4, H and I). Interestingly, we observed that a small but significant portion of DCs migrating to *TNFΔARE* MLNs trafficked in a CCR7-independent manner (Figure 4I).

Discussion

We report the striking formation of mesenteric TLOs and other mesenteric and mucosal lymphatic abnormalities associated with the chronic ileal inflammation of the *TNFΔARE* mouse model. Thus far, TLOs have only been identified in the mucosa of experimentally inflamed ileum. The limited characterization provided in these studies[10–13] does not allow us to confidently confirm whether these structures are true TLOs or gut-associated lymphoid follicles. Our study presents a detailed characterization of mesenteric TLOs in *TNFΔARE* mice (Supplemental Figure S2), which are geographically distinct from mucosal TLOs previously described in this model,[25] and offers key insights into their function. Our findings suggest that mesenteric TLOs appear with disease progression because these structures were not detected in mesenteries from mice younger than 16 weeks; however, their developmental course needs to be studied in more detail. Importantly, formation of these mesenteric TLOs suggests a persistent inflammation in this tissue, a feature that has not been examined in the context of CD. In this regard, the observation that TLOs not only appear where the main mesenteric collecting vessels normally lie but also are found in the nearby mesothelium normally devoid of such vessels is of interest because it suggests that immunoreactive cells and antigens are somehow reaching these areas and dictate the formation of these local immune centers. Consistent with this theory is our finding that collecting lymphatic vessels, normally able to restrict lymph-borne antigens to their lumen, are leaky in *TNFΔARE* mice, thereby potentially spilling their lymph content into nearby tissue.

Using the fluorescent lipid bodipy as a marker, we observed increased lipid clearance from *TNFΔARE* feces and ileum and increased accumulation in MLNs and blood. Although in this inflammatory situation, lipid absorption and accumulation could be modulated by potential changes in gut motility and lymph node hydrodynamics, our findings suggest increased transport of lipid from the gut lumen to MLN and blood and an overall increase in lymph production and drainage via mesenteric lymphatic vessels. Increased lymph formation would be consistent with the significant submucosal edema and granulomas observed within the *TNFΔARE* lamina propria. We also found that intestinal lacteals and submucosal lymphatics undergo robust expansion, suggesting another compensatory response of the lymphatic system to deal with increased antigen load and interstitial fluid during chronic inflammation. However, these newly established vessels may be dysfunctional because they appear tortuous and disorganized, a feature consistently reported in clinical immunohistochemical studies.[7,26,27] Furthermore, we found that these vessels are leaky, as suggested by bodipy droplets accumulating in the mesentery surrounding the lymphatic vessels. Considering that the inflamed mesentery is exposed to a soup of inflammatory agents that could increase vessel permeability,[28] these data are not surprising. Taken together, our findings suggest that the chronic inflammation and unresolved submucosal edema in *TNFΔARE* mice can continue to drive increased lymph flow from the inflamed ileum, despite disorganized newly formed intestinal lymphatics and leaky mesenteric collectors.

We further confirmed increased lymph flow in mesenteric *TNFΔARE* by mechanistically demonstrating that naive and intestinally derived DCs have an enhanced ability to traffic to mesenteric MLNs. Such increased DC numbers in inflamed MLNs have been consistently associated with CD pathogenesis.[29–31] We also revealed an important role for CCL21/CCR7 in the DC trafficking process; albeit, we saw a small but significant CCR7-independent DC trafficking to *TNFΔARE* MLNs, an observation similar to that previously shown in models of skin and blood inflammation.[32,33] Increases in CCL21 expression along the mesenteric lymphatic vessels from the gut to the MLN were seen in inflamed tissues. This first report of CCL21 expression by mesenteric collecting lymphatic vessels suggests that DC migration to draining lymph nodes could be facilitated by a gradient formed by the chemokine, as recently suggested.[34]

Importantly, our data highlight important trafficking of DCs to mesenteric TLOs, with, enrichment in CX_3CR_1-expressing DC subsets, compared with MLNs. Thus, our findings implicate a differential, proinflammatory role of DCs within these organs and provide a foundation for further experiments that will offer more clues as to the modulatory role, if any, of mesenteric TLOs in chronic inflammation.

A main question remaining unanswered is whether mesenteric TLOs play a proinflammatory or proresolution role during ileitis. In models of microbial infection, TLOs appear to act as reservoirs of pathogens, preventing them from systemically spreading.[35,36] TLOs may also provide an additional location for B-cell proliferation, potentiating the immune response during inflammation.[37,38] A recent study suggested TLOs as a proresolving mechanism during inflammation that facilitates lymphocyte egress.[39] Another emerging consideration is that lymphoid neogenesis is a response to defective lymphatic drainage and persistent antigen exposure.[40] This theory proposes that TLOs provide a detour for antigens, further adding to the immune insult to the tissue. Indeed, we observe leaky lymphatic vessels that might be unable to properly distribute antigens

to draining lymph nodes. We hypothesize that the lymph, leaking from lymphatic vessels, is the source of the many signaling molecules involved in TLO neogenesis and possible lymphangiogenesis; however, this needs to be further examined.

Importantly, a newly published study reported the development of lymphoid aggregates in the ileal mesentery of patients with CD,[41] which were described as distributed along and impinged on lymphatic collecting vessels, bearing striking similarities with the TLOs we describe here. These findings solidify our observations of mesenteric TLOs in *TNFΔARE* mice and validate this animal model as a reliable, critically needed, model to study CD pathophysiology.

Acknowledgments

We thank Dr. Frank Jirik for generously providing us with *TNFΔARE* breeding pairs; Laurie Alston and Simon Roizes for their excellent technical help; and Dr. Karen Poon for her flow cytometry services within the Snyder Institute for Chronic Diseases at the University of Calgary, Calgary, Alberta, Canada.

Supplemental Data

Supplemental material for this article can be found at *http://dx.doi.org/10.1016/j.ajpath.2016.12.007*.

References

1. Kirsner JB: Observations on the etiology and pathogenesis of inflammatory bowel disease. Edited by Bockus H. In Gastroenterology. Philadelphia: Saunders, 1976. pp. 521−539
2. Kovi J, Duong HD, Hoang CT: Ultrastructure of intestinal lymphatics in Crohn's disease. Am J Clin Pathol 1981, 76:385−394
3. Robb-Smith AH: A bird's-eye view of Crohn's disease. Proc R Soc Med 1971, 64:157−161
4. Crohn BB, Ginzburg L, Oppenheimer GD: Regional ileitis, a pathological and clinical entity. J Am Med Ass 1932, 99:1323−1328
5. Kalima TV: The structure and function of intestinal lymphatics and the influence of impaired lymph flow on the ileum of rats. Scand J Gastroenterol Suppl 1971, 10:1−87
6. Heatley RV, Bolton PM, Hughes LE, Owen EW: Mesenteric lymphatic obstruction in Crohn's disease. Digestion 1980, 20:307−313
7. Pedica F, Ligorio C, Tonelli P, Bartolini S, Baccarini P: Lymphangiogenesis in Crohn's disease: an immunohistochemical study using monoclonal antibody D2-40. Virchows Arch 2008, 452: 57−63
8. D'Alessio S, Correale C, Tacconi C, Gandelli A, Pietrogrande G, Vetrano S, Genua M, Arena V, Spinelli A, Peyrin-Biroulet L, Fiocchi C, Danese S: VEGF-C-dependent stimulation of lymphatic function ameliorates experimental inflammatory bowel disease. J Clin Invest 2014, 124:3863−3878
9. Alexander JS, Chaitanya GV, Grisham MB, Boktor M: Emerging roles of lymphatics in inflammatory bowel disease. Ann N Y Acad Sci 2010, 1207 Suppl 1:E75−E85
10. Collins CB, Aherne CM, McNamee EN, Lebsack MD, Eltzschig H, Jedlicka P, Rivera-Nieves J: Flt3 ligand expands CD103(+) dendritic cells and FoxP3(+) T regulatory cells, and attenuates Crohn's-like murine ileitis. Gut 2012, 61:1154−1162
11. Kaiserling E: Newly-formed lymph nodes in the submucosa in chronic inflammatory bowel disease. Lymphology 2001, 34:22−29
12. Kobayashi M, Mitoma J, Nakamura N, Katsuyama T, Nakayama J, Fukuda M: Induction of peripheral lymph node addressin in human gastric mucosa infected by Helicobacter pylori. Proc Natl Acad Sci U S A 2004, 101:17807−17812
13. Surawicz CM, Belic L: Rectal biopsy helps to distinguish acute self-limited colitis from idiopathic inflammatory bowel disease. Gastroenterology 1984, 86:104−113
14. Aloisi F, Pujol-Borrell R: Lymphoid neogenesis in chronic inflammatory diseases. Nat Rev Immunol 2006, 6:205−217
15. Torkzad MR, Ullberg U, Nystrom N, Blomqvist L, Hellstrom P, Fagerberg UL: Manifestations of small bowel disease in pediatric Crohn's disease on magnetic resonance enterography. Inflamm Bowel Dis 2012, 18:520−528
16. Tarjan Z, Toth G, Gyorke T, Mester A, Karlinger K, Mako EK: Ultrasound in Crohn's disease of the small bowel. Eur J Radiol 2000, 35: 176−182
17. Benmiloud S, Chaouki S, Atmani S, Hida M: Multicentric Castleman's disease in a child revealed by chronic diarrhea. Case Rep Pediatr 2015, 2015:689206
18. Kontoyiannis D, Pasparakis M, Pizarro TT, Cominelli F, Kollias G: Impaired on/off regulation of TNF biosynthesis in mice lacking TNF AU-rich elements: implications for joint and gut-associated immunopathologies. Immunity 1999, 10:387−398
19. Elsheikh W, Flannigan KL, McKnight W, Ferraz JG, Wallace JL: Dextran sulfate sodium induces pan-gastroenteritis in rodents: implications for studies of colitis. J Physiol Pharmacol 2012, 63: 463−469
20. Rehal S, von der Weid PY: Experimental ileitis alters prostaglandin biosynthesis in mesenteric lymphatic and blood vessels. Prostaglandins Other Lipid Mediat 2015, 116−117:37−48
21. Mathias R, von der Weid PY: Involvement of the NO-cGMP-K(ATP) channel pathway in the mesenteric lymphatic pump dysfunction observed in the guinea pig model of TNBS-induced ileitis. Am J Physiol Gastrointest Liver Physiol 2013, 304: G623−G634
22. Rehal S, Blanckaert P, Roizes S, von der Weid PY: Characterization of biosynthesis and modes of action of prostaglandin E2 and prostacyclin in guinea pig mesenteric lymphatic vessels. Br J Pharmacol 2009, 158: 1961−1970
23. von der Weid PY, Muthuchamy M: Regulatory mechanisms in lymphatic vessel contraction under normal and inflammatory conditions. Pathophysiology 2010, 17:263−276
24. Von Der Weid PY, Rehal S: Lymphatic pump function in the inflamed gut. Ann N Y Acad Sci 2010, 1207 Suppl 1:E69−E74
25. McNamee EN, Masterson JC, Jedlicka P, Collins CB, Williams IR, Rivera-Nieves J: Ectopic lymphoid tissue alters the chemokine gradient, increases lymphocyte retention and exacerbates murine ileitis. Gut 2013, 62:53−62
26. Kenney BC, Jain D: Identification of lymphatics within the colonic lamina propria in inflammation and neoplasia using the monoclonal antibody D2-40. Yale J Biol Med 2008, 81:103−113
27. Rahier JF, De Beauce S, Dubuquoy L, Erdual E, Colombel JF, Jouret-Mourin A, Geboes K, Desreumaux P: Increased lymphatic vessel density and lymphangiogenesis in inflammatory bowel disease. Aliment Pharmacol Ther 2011, 34:533−543
28. Cromer WE, Zawieja SD, Tharakan B, Childs EW, Newell MK, Zawieja DC: The effects of inflammatory cytokines on lymphatic endothelial barrier function. Angiogenesis 2014, 17:395−406
29. Baumgart DC, Metzke D, Guckelberger O, Pascher A, Grotzinger C, Przesdzing I, Dorffel Y, Schmitz J, Thomas S: Aberrant plasmacytoid dendritic cell distribution and function in patients with Crohn's disease and ulcerative colitis. Clin Exp Immunol 2011, 166: 46−54

30. Magnusson MK, Brynjolfsson SF, Dige A, Uronen-Hansson H, Borjesson LG, Bengtsson JL, Gudjonsson S, Ohman L, Agnholt J, Sjovall H, Agace WW, Wick MJ: Macrophage and dendritic cell subsets in IBD: ALDH+ cells are reduced in colon tissue of patients with ulcerative colitis regardless of inflammation. Mucosal Immunol 2016, 9:171−182
31. Mottet C, Uhlig HH, Powrie F: Cutting edge: cure of colitis by CD4+CD25+ regulatory T cells. J Immunol 2003, 170:3939−3943
32. Vigl B, Aebischer D, Nitschke M, Iolyeva M, Rothlin T, Antsiferova O, Halin C: Tissue inflammation modulates gene expression of lymphatic endothelial cells and dendritic cell migration in a stimulus-dependent manner. Blood 2011, 118:205−215
33. Nakano H, Lin KL, Yanagita M, Charbonneau C, Cook DN, Kakiuchi T, Gunn MD: Blood-derived inflammatory dendritic cells in lymph nodes stimulate acute T helper type 1 immune responses. Nat Immunol 2009, 10:394−402
34. Randolph GJ, Angeli V, Swartz MA: Dendritic-cell trafficking to lymph nodes through lymphatic vessels. Nat Rev Immunol 2005, 5:617−628
35. Ghosh S, Steere AC, Stollar BD, Huber BT: In situ diversification of the antibody repertoire in chronic Lyme arthritis synovium. J Immunol 2005, 174:2860−2869
36. Steere AC, Duray PH, Butcher EC: Spirochetal antigens and lymphoid cell surface markers in Lyme synovitis. Comparison with rheumatoid synovium and tonsillar lymphoid tissue. Arthritis Rheum 1988, 31: 487−495
37. Dorner T, Hansen A, Jacobi A, Lipsky PE: Immunglobulin repertoire analysis provides new insights into the immunopathogenesis of Sjogren's syndrome. Autoimmun Rev 2002, 1:119−124
38. Schroder AE, Greiner A, Seyfert C, Berek C: Differentiation of B cells in the nonlymphoid tissue of the synovial membrane of patients with rheumatoid arthritis. Proc Natl Acad Sci U S A 1996, 93: 221−225
39. Nayar S, Campos J, Chung MM, Navarro-Nunez L, Chachlani M, Steinthal N, Gardner DH, Rankin P, Cloake T, Caamano JH, McGettrick HM, Watson SP, Luther S, Buckley CD, Barone F: Bimodal expansion of the lymphatic vessels is regulated by the sequential expression of IL-7 and lymphotoxin alpha1beta2 in newly formed tertiary lymphoid structures. J Immunol 2016, 197: 1957−1967
40. Thaunat O, Kerjaschki D, Nicoletti A: Is defective lymphatic drainage a trigger for lymphoid neogenesis? Trends Immunol 2006, 27:441−445
41. Randolph GJ, Bala S, Rahier JF, Johnson MW, Wang PL, Nalbantoglu I, Dubuquoy L, Chau A, Pariente B, Kartheuser A, Zinselmeyer BH, Colombel JF: Lymphoid aggregates remodel lymphatic collecting vessels that serve mesenteric lymph nodes in Crohn disease. Am J Pathol 2016, 186:3066−3073